J Phys. F: Metal Phys., Vol. 6, No. 5, 1976. Printed in Great Britain.

Electrical resistivity of ferromagnetic nickel and iron based alloys

A Fert and I A Campbell
Laboratoire de Physique des Solides†, Université de Paris-Sud, 91405 Orsay

Received 1 December 1975

Abstract. We discuss in detail the theoretical basis for the two-band model with spin-mixing which has been widely applied to the analysis of the transport properties of ferromagnetic metals. This model is shown to have much more general validity than the original presentation suggested. The model is then applied to resistivity data in Ni and Fe based alloys to obtain a consistent set of parameters for the scattering within each spin band for various impurities, together with temperature dependent pure metal scattering rates.

1. Introduction

Following Mott's ideas (Mott 1964), we showed some years ago that several transport properties of nickel and iron based ferromagnetic alloys can be explained by assuming conduction in parallel by the spin up and spin down electrons (Campbell *et al* 1967, Fert and Campbell 1968, 1971). The physical basis of this two current model is the dominance of spin-conserving scattering and the weakness of the spin-flip collisions in a ferromagnetic alloy at low temperature. This two current model was taken up by many authors, developed in several directions and sometimes criticized: we refer chiefly to Farrell and Greig (1968), Durand and Gautier (1970), Schwerer and Conroy (1971), Price and Williams (1973), Greig and Rowlands (1974), Dorleijn and Miedema (1975), Jaoul and Campbell (1975) for studies on Ni based alloys and to the work of Loegel and Gautier (1971) on Co based alloys. It seems that the different scattering of the spin ↑ and spin ↓ electrons has been generally confirmed and that the various papers are nearly in agreement as to the ratios $\alpha = \rho_{0\downarrow}/\rho_{0\uparrow}$ of the spin ↑ and spin ↓ resistivities $\rho_{0\uparrow}$ and $\rho_{0\downarrow}$ induced by a given impurity in a given host. On the contrary, opinions are divided as to the occurrence of a temperature-dependent spin-mixing mechanism which would result from scattering by spin waves and would tend to equalize the currents as the temperature is raised, some authors preferring the idea of two independent currents at all temperatures.

In this paper, we report some resistivity measurements on Ni and Fe based alloys and we also review the general pattern of the electrical conduction in these ferromagnetic alloys.

In §2, we place the two current and spin-mixing model on a more solid theoretical basis. In particular, it is shown that the conduction electrons of nickel are far from

† Laboratoire associé au CNRS.

being free electrons (e.g. from the cyclotron resonance performed by Goy and Grimes 1973) and an extension of the previous models to band electrons is needed.

In §3, we describe the experimental procedure used to obtain the results reported in §§4, 5 and 6.

In §4, we report measurements of the residual resistivity of ternary dilute alloys $Ni_{1-x-y}A_xB_y$ and the analysis of the deviations from Matthiessen's rule (MR). This type of study which we introduced for Fe based alloys (Campbell *et al* 1967) has also been done on Ni based alloys by Leonard *et al* (1969) and by Dorleijn and Miedema (1975) and allows a straightforward determination of the impurity resistivities for the spin ↑ and spin ↓ electrons. We interpret the spin ↑ and spin ↓ resistivities of transition impurities on the Friedel model for the ferromagnetic transition alloys.

In §5, we report experimental results on the temperature dependence of the resistivity of $Ni_{1-x}T_x$ alloys (where T is a transition metal, $7 \times 10^{-4} < x < 3 \times 10^{-2}$). The deviations from MR at low temperature are approximately independent of the concentration when the residual resistivity is large enough ($\rho_0 \gtrsim 1\ \mu\Omega\,\text{cm}$) and can be then interpreted fairly well in the two current model. We argue the need of a spin mixing by spin waves to explain the results.

In §6, we report measurements of the temperature dependence of the resistivity of iron based dilute alloys and discuss their interpretation in the two current model.

The two current model has also been used to interpret other transport properties of ferromagnetic alloys: thermo–electric power (Cadeville *et al* 1969, Farrell and Greig 1970), spontaneous anisotropy of resistivity (Campbell *et al* 1970), extraordinary Hall effect (Fert and Jaoul 1972). However, the discussion of these transport properties is not in the scope of this paper and we shall only consider the experimental data concerning the resistivity and its temperature dependence.

2. Model for two current conduction with inter-current scattering

Two current (or two band) models have often been used to describe the electrical conduction in metals. One assumes that two groups of electrons (e.g. belly and neck electrons) carry current *independently* in parallel, which means that one neglects the momentum transfer by scattering from one to the other group.

In ferromagnetic alloys, we separate the electrons into two groups in the same way, but here the groups are spin ↑ and spin ↓ electrons, as scattering with conservation of spin can certainly be assumed to dominate, at least at low temperatures†. We will however improve on the traditional two current models by including the transfer of momentum between the two groups of electrons by spin-flip scattering. We present in this section a model which describes this conduction by two coupled currents. This model provides a generalized justification for a simpler previous model which assumed a conduction band of quasi-free electrons (Campbell *et al* 1967, Fert 1969).

We recall first how the resistivity can be calculated by using the variational method (Ziman 1960). In the notation of Ziman the Boltzmann equation can be written

$$X = P\psi(\boldsymbol{k}\sigma) \tag{1}$$

† As usual, we call spin ↑ the majority spin direction. Note that the separation of the conduction electrons into two groups according to their spin is justified only if the mean free path is much shorter than the size of the magnetic domains. This condition is generally fulfilled except for very pure metals.

where P is the scattering operator and where $\psi(\boldsymbol{k}\sigma)$ is the extra-energy distribution defined by

$$f(\boldsymbol{k}\sigma) = f^0(\epsilon_k) - \psi(\boldsymbol{k}\sigma)(\partial f^0/\partial \epsilon_k). \tag{2}$$

The variational principle (Ziman 1960) leads to the determination of $\psi(\boldsymbol{k}\sigma)$ by minimizing

$$\frac{\langle \psi, P\psi \rangle}{(\langle \psi, X \rangle)^2}. \tag{3}$$

The electrons being divided into two groups according to their spin σ, we choose a trial function $\psi(\boldsymbol{k}\sigma)$ in the form of a linear combination of two functions $\phi_\sigma(\boldsymbol{k})$ ($\sigma = \pm\frac{1}{2}$):

$$\psi(\boldsymbol{k}\sigma) = \eta_\sigma \phi_\sigma(\boldsymbol{k}) \tag{4}$$

or

$$\psi(\boldsymbol{k}\sigma) = \sum_{\sigma'} \eta_{\sigma'} \phi_{\sigma'}(\boldsymbol{k})\, \delta_{\sigma\sigma'}. \tag{5}$$

The distributions $\phi_\uparrow(\boldsymbol{k})$ and $\phi_\downarrow(\boldsymbol{k})$ are supposed known and independent of the scattering process, while the coefficients $\eta_\uparrow$ and $\eta_\downarrow$ have to be adjusted to minimize (3). This is the implicit hypothesis for almost all two current models: the distribution of relaxation rate within a given electron group is supposed independent of the scatterer type but the relative relaxation of the two groups depends on the scatterer.

The values of η_σ which minimize (3) are given (Ziman 1960) by the equations

$$\mathscr{E} X_\sigma = \sum_{\sigma'} P_{\sigma\sigma'} \eta_{\sigma'} \tag{6}$$

with

$$X_\sigma = -\int (\boldsymbol{v}_k \cdot \boldsymbol{u})\, e \frac{\partial f^0}{\partial \epsilon_k} \Phi_\sigma(\boldsymbol{k})\, \mathrm{d}\boldsymbol{k} \tag{7}$$

$$P_{\sigma\sigma'} = \frac{1}{2k_B T} \sum_{\sigma''\sigma'''} [\phi_\sigma(\boldsymbol{k})\, \delta_{\sigma\sigma''} - \phi_\sigma(\boldsymbol{k}')\, \delta_{\sigma\sigma'''}] P(\boldsymbol{k}_{\sigma''} \boldsymbol{k}'_{\sigma'''}) \times [\phi_{\sigma'}(\boldsymbol{k})\, \delta_{\sigma'\sigma''} - \phi_{\sigma'}(\boldsymbol{k}')\, \delta_{\sigma'\sigma'''}]\, \mathrm{d}\boldsymbol{k}\, \mathrm{d}\boldsymbol{k}' \tag{8}$$

where $\boldsymbol{u}$ is the unit vector in the direction of the electric field and where $P(\boldsymbol{k}\sigma'', \boldsymbol{k}'\sigma''')$ is the equilibrium rate between the states $(\boldsymbol{k}\sigma'')$ and $(\boldsymbol{k}'\sigma''')$.

The resistivity ρ is then given (Ziman 1960) by

$$\rho^{-1} = \sum_{\sigma\sigma'} X_\sigma (P^{-1})_{\sigma\sigma'} X_{\sigma'}. \tag{9}$$

If we define

$$\rho_\uparrow = \frac{P_{\uparrow\uparrow}}{X_\uparrow^2} + \frac{P_{\downarrow\downarrow}}{X_\uparrow X_\downarrow} \tag{10}$$

$$\rho_\downarrow = \frac{P_{\downarrow\downarrow}}{X_\downarrow^2} + \frac{P_{\uparrow\downarrow}}{X_\uparrow X_\downarrow} \tag{11}$$

$$\rho_{\uparrow\downarrow} = -\frac{P_{\uparrow\downarrow}}{X_\uparrow X_\downarrow} \tag{12}$$

one obtains

$$\rho = \frac{\rho_\uparrow\rho_\downarrow + \rho_{\uparrow\downarrow}(\rho_\uparrow\rho_\downarrow)}{\rho_\uparrow + \rho_\downarrow + 4\rho_{\uparrow\downarrow}}. \tag{13}$$

This equation for the resistivity has been already found in the case of two equal groups of free electrons (Campbell *et al* 1967, Fert 1969). The interest of the present derivation is to show that this simple expression for the resistivity is quite general, and that the resistivity in a two-band model including inter-band scattering is always given by an expression of the form (13) with the parameters ρ_σ, $\rho_{\uparrow\downarrow}$ defined by the equations (10) to (12). In fact, although our interest at present is ferromagnetic metals, this expression would apply equally well if the two groups of electrons were for instance the 'neck' and 'belly' electrons of a noble metal. We point out that, after (10), (11) and (12), the resistivities $\rho_\uparrow$, $\rho_\downarrow$ and $\rho_{\uparrow\downarrow}$ depend linearly on the scattering operator, so that different scattering processes provide additive contributions to the three resistivities. This justifies the application of Mathiessen's rule for $\rho_\uparrow$, $\rho_\downarrow$ and $\rho_{\uparrow\downarrow}$. This property results from the assumption that $\phi_\sigma(\boldsymbol{k})$ is independent of the scatterer type.

In the absence of spin-flip collisions ($P(\boldsymbol{k}_\uparrow, \boldsymbol{k}'_\downarrow) = 0$), $\rho_{\uparrow\downarrow}$ cancels out and one obtains the classical expression of the resistivity in a model with two independent currents

$$\rho = \frac{\rho_\uparrow\rho_\downarrow}{\rho_\uparrow + \rho_\downarrow}. \tag{14}$$

Approximate but practical expressions for $\rho_\uparrow$, $\rho_\downarrow$ and $\rho_{\uparrow\downarrow}$ are obtained if one chooses:

$$\phi_\uparrow(\boldsymbol{k}) = \phi_\downarrow(\boldsymbol{k}) = \boldsymbol{k}.\boldsymbol{u}. \tag{15}$$

($\boldsymbol{k}.\boldsymbol{u}$ is the extra-energy distribution for a spherical Fermi surface and a scattering probability depending only on the scattering angle.) One obtains:

$$\rho_\sigma = \frac{1}{X_\sigma^2 k_B T} \sum_{\sigma'} \int (\boldsymbol{k}.\boldsymbol{u})[(\boldsymbol{k} - \boldsymbol{k}').\boldsymbol{u}]P(\boldsymbol{k}\sigma, \boldsymbol{k}'\sigma')\,\mathrm{d}\boldsymbol{k}\,\mathrm{d}\boldsymbol{k}' \tag{16}$$

$$\rho_{\uparrow\downarrow} = \frac{1}{X_\uparrow X_\downarrow k_B T} \int (\boldsymbol{k}.\boldsymbol{u})(\boldsymbol{k}'.\boldsymbol{u})P(\boldsymbol{k}_\uparrow, \boldsymbol{k}'_\downarrow)\,\mathrm{d}\boldsymbol{k}\,\mathrm{d}\boldsymbol{k}'. \tag{17}$$

The expression (16) for ρ_σ is a classical resistivity expression derived by the variational method (Ziman 1960). Both spin flip and non-spin flip transitions contribute to ρ_σ. It can be remarked that expression (16) for ρ_σ contains the factor $(\boldsymbol{k} - \boldsymbol{k}').\boldsymbol{u}$ which involves the momentum transferred to the lattice in the transition $\boldsymbol{k} \rightarrow \boldsymbol{k}'$, whereas this factor is replaced in expression (17) for $\rho_{\uparrow\downarrow}$ by $\boldsymbol{k}'.\boldsymbol{u}$ which involves the momentum gained by the final spin direction.

Two current models for ferromagnetic alloys have generally assumed that the two electrons groups are constituted by the spin $\uparrow$ and spin $\downarrow$s electrons and that the d electrons carry a negligible current. However, according to recent data on the band structure and on the s–d hybridization the difference of effective mass between the d and the 's' electrons (with d hybridization) is less marked than it was generally assumed. In our model we suppose that the band of spin σ includes all the electrons with spin σ, with s, d or hybridized character. Stopping at this stage (equation 13), rather than trying to treat the true 'many band' conductor, is meaningful if the additivity rule for the parameters $\rho_\uparrow$, $\rho_\downarrow$ and $\rho_{\uparrow\downarrow}$ is reasonably well obeyed. In practice the rule will remain valid if changes in scatterer produce

much weaker effects on the distribution of scattering rates over the Fermi surface than on the ratio of spin ↑ to spin ↓ scattering. If the interband scattering is relatively weak, the dominant mechanism of deviation from MR will then result from the two current conduction.

We can consider briefly the case of Ni. Fermi surface calculations and measurements (Goy and Grimes 1973, Tsui 1967, Wang and Callaway 1974) show that the clear distinction of the simple s–d model between heavy d electron states and light sp states is an over-simplification; there are in reality light $d_\downarrow$ orbits near the point X while some $sp_\downarrow$ band orbits are quite heavy. For the spin ↑ states, the neck orbits are particularly light. In addition, in the presence of impurities we should also consider the different scattering probabilities for different parts of the Fermi surface. In practice, these complicated effects will be hidden inside $\rho_\uparrow$ and $\rho_\downarrow$.

The existence of a spin–orbit effect poses a different problem. Realistic ferromagnetic metal band structures (Wang and Callaway 1974) show Fermi surface regions of hybridized spin ↑ and spin ↓ character. How does this affect the two band approach? We can still include this in the formalism—we can arbitrarily draw the line between spin ↑ and spin ↓ somewhere in the hybridized region, and scatterings across this boundary will contribute both to ρ_σ and to $\rho_{\uparrow\downarrow}$. It is important to remember the existence of this type of contribution to $\rho_{\uparrow\downarrow}$ in the interpretation of experimental results.

We want to conclude this section by a discussion of the several mechanisms of spin-mixing in ferromagnetic Ni or Fe based alloys. Spin-flip occurs first in the collisions with spin waves. This mechanism induces a resistivity $\rho_{\uparrow\downarrow}(T)$ of which the order of magnitude is that indicated by the experimental data (Fert 1969) and is considered as the principal mechanism of spin-mixing. Another contribution to $\rho_{\uparrow\downarrow}(T)$ comes from collisions between spin ↑ and spin ↓ electrons but has been shown to be negligible (Bourguart *et al* 1968). The spin-mixing term induced by spin wave scattering (and also the electron collisions) vanishes at 0 K, but there is also a residual spin-mixing. First, there is a spin-flip scattering by the impurities due to the spin–orbit coupling, but from EPR data (Monod 1968) the spin-flip cross section of a 3d impurity in Cu is about 100 times smaller than its non-spin flip cross section. The same order of magnitude is expected for the spin-flip cross section of the 3d impurities in Ni or Fe, so that the residual term $\rho_{\uparrow\downarrow}(0)$ induced by this mechanism should be negligible. In fact we have conventionally taken the impurity spin flip scattering to be zero throughout—the effect of a small impurity spin flip term is probably indistinguishable from small changes in the apparent values of ρ_σ for that impurity.

Spin-mixing at 0 K can also result from the combined action of the internal magnetic induction and of the spin–orbit coupling. The resulting spin mixing term is independent of the concentration of impurities and so is only effective in alloys of low residual resistivity. A zero temperature term $\rho_{\uparrow\downarrow}(0)$ introduced phenomenologically explains the behaviour of a number of experimental parameters in dilute alloys in which the residual resistivity is below about 1 $\mu\Omega$ cm (Jaoul and Campbell 1975).

In this paper we concentrate on alloys in the concentration range where the residual spin-mixing can be neglected.

3. Experimental

The alloys were prepared at the CEN Grenoble in a levitation furnace with base metal obtained by zone melting (RRR = 700 and 25 for Ni and Fe respectively). The

alloys were drawn into wires of diameter 1 mm and annealed at 900°C for the Ni based alloys, 800°C for the iron based alloys. The absence of precipitates was checked by micrography. Most of the binary alloys and all the ternary alloys were analysed by colorimetry or atomic absorption spectrophotometry.

The resistivity was measured between 1·3 K and 77 K and at several temperatures between 77 K and 300 K by a classical DC method (potentiometer + nanovoltmeter). The accuracy of the resistance measurement was generally limited (except for the less concentrated alloys) by the stability of the current ($\pm 2 \times 10^{-5}$). The temperature in the helium range was measured by a germanium resistor with an accuracy of 0·1 K.

4. Residual resistivity of ternary dilute alloys

If the residual spin-mixing is neglected (see discussion at the end of §2), the spin ↑ and spin ↓ electrons of ferromagnetic alloys carry the current independently in the low temperature limit. The residual resistivity of a binary dilute alloy **MA** is then

$$\rho_A = C_A \frac{\rho_{A\uparrow}\rho_{A\downarrow}}{\rho_{A\uparrow} + \rho_{A\downarrow}} \tag{18}$$

where C_A is the concentration of impurities A and where $C_A\rho_{A\uparrow}$ and $C_A\rho_{A\downarrow}$ are the residual resistivities for each spin direction.

We consider now a ternary alloy **MAB** containing a concentration C_A of impurities A and C_B of impurities B. If we suppose that the impurities A and B add their resistivity in each current ($\rho_\sigma = C_A\rho_{A\sigma} + C_B\rho_{B\sigma}$), the model predicts a deviation of the alloy residual resistivity from Mathiessen rule:

$$\Delta\rho = \rho_{AB} - (\rho_A + \rho_B) = \frac{(\alpha_A - \alpha_B)^2\rho_A\rho_B}{(1 + \alpha_A)^2\alpha_B\rho_A + (1 + \alpha_B)^2\alpha_A\rho_B} \tag{19}$$

where $\alpha_A = \rho_{A\downarrow}/\rho_{A\uparrow}$ and $\alpha_B = \rho_{B\downarrow}/\rho_{B\uparrow}$. The analysis of the deviations from MR in alloys **MAB** with several proportions of A and B can be used to determine α_A and α_B.

We have measured the residual resistivity of binary $\mathbf{Ni}_{1-x}\mathbf{A}_x$ and ternary $\mathbf{Ni}_{1-x-y}\mathbf{A}_x\mathbf{B}_y$ alloys ($7 \times 10^{-4} < x$ or $y < 3 \times 10^{-2}$, A or B = Co, Fe, Mn, Cr, V, Ti). The residual resistivity of most of the alloys was sufficient for the residual spin-mixing to be neglected.

From the measurements on binary alloys we have determined the residual resistivity per at% of various impurities. Then we have measured the residual resistivity of ternary alloys and observed clear deviations from MR which are shown on figure 1 for **NiVCo**, **NiVFe**, **NiCrMn** and **NiCrTi** alloys. We found a set of parameters α_i to fit the experimental results. The best fit has been obtained with the values α given in table 1† and the agreement between the calculated and experimental points can be seen on figure 1‡. We note that most impurities can be separated into a first group (Co, Fe, Mn) with very high values of α and a second group (Cr, V) for which α is smaller than one. This explains the large deviations from MR for ternary alloys containing an element of each group (e.g. **NiCoV**). On the contrary the

† We have chosen the set of parameters given in table 1 rather than the set α^{-1} as being more consistent with the electronic structure of the impurities.

‡ A technique for estimating α values unambiguously from such data is given in the Appendix.

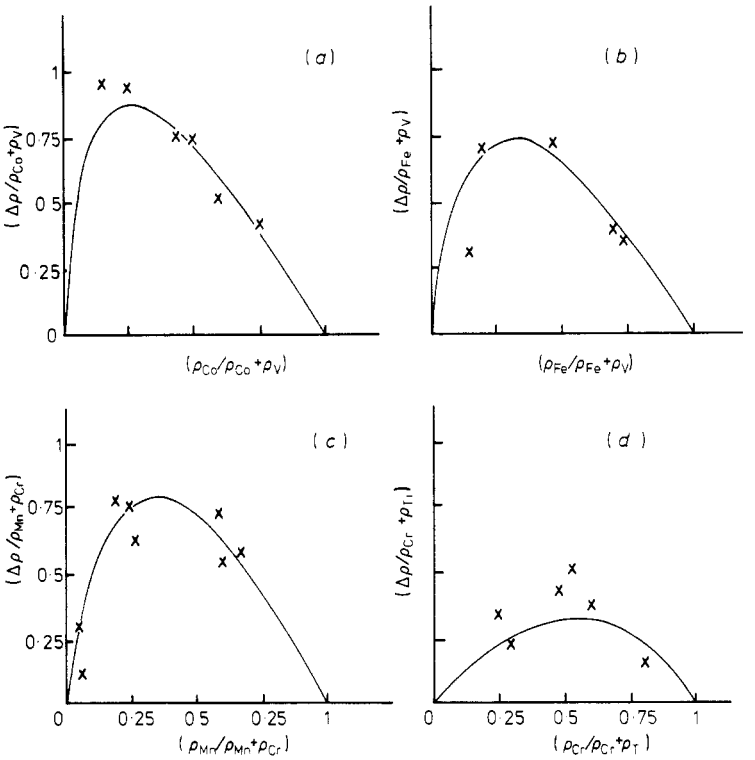

Figure 1. Deviations from Matthiessen's rule in Ni based ternary alloys (relative deviations against relative resistivities). (*a*), **Ni**CoV; (*b*), **Ni**FeV; (*c*), **Ni**MnCr; (*d*), **Ni**CrTi. The full curves are calculated from expression (19) with the values of α listed in table 1.

deviations are negligible when both impurities have nearly the same ratio α (this has also been observed by Dorleijn and Miedema (1975)). The latter result shows that additional deviations from MR induced, for instance, by the anisotropy of the relaxation on the Fermi surface are much smaller than the deviations linked with the spin dependent scattering.

The results for the spin ↑ and spin ↓ resistivities of the impurities

$$\rho_{A\uparrow} = \frac{1}{1+\alpha_A}\rho_A \qquad \rho_{A\downarrow} = \frac{\alpha_A}{1+\alpha_A}\rho_A$$

Table 1. The residual resistivity per at%, the parameter $\alpha = \rho_{0\downarrow}/\rho_{0\uparrow}$ and the spin ↑ and spin ↓ residual resistivities per at% for 3d impurities in nickel.

Impurity	Ti	V	Cr	Mn	Fe	Co
Resistivity ρ_0(μΩ cm/at%)	2·9	4·5	5·0	0·61	0·35	0·145
$\alpha = \rho_{0\downarrow}/\rho_{0\uparrow}$	4 ($3 < \alpha < 5$)	0·55 ($0{\cdot}5 < \alpha < 0{\cdot}6$)	0·45 ($0{\cdot}35 < \alpha < 0{\cdot}5$)	15 ($11{\cdot}5 < \alpha < 17$)	20 ($15 < \alpha < 23$)	30 ($23 < \alpha < 33$)
$\rho_{0\uparrow}$(μΩ cm/at%)	3·6	12·7	16·1	0·65	0·37	0·15
$\rho_{0\downarrow}$(μΩ cm/at%)	14·5	7·0	7·2	9·8	7·4	4·6

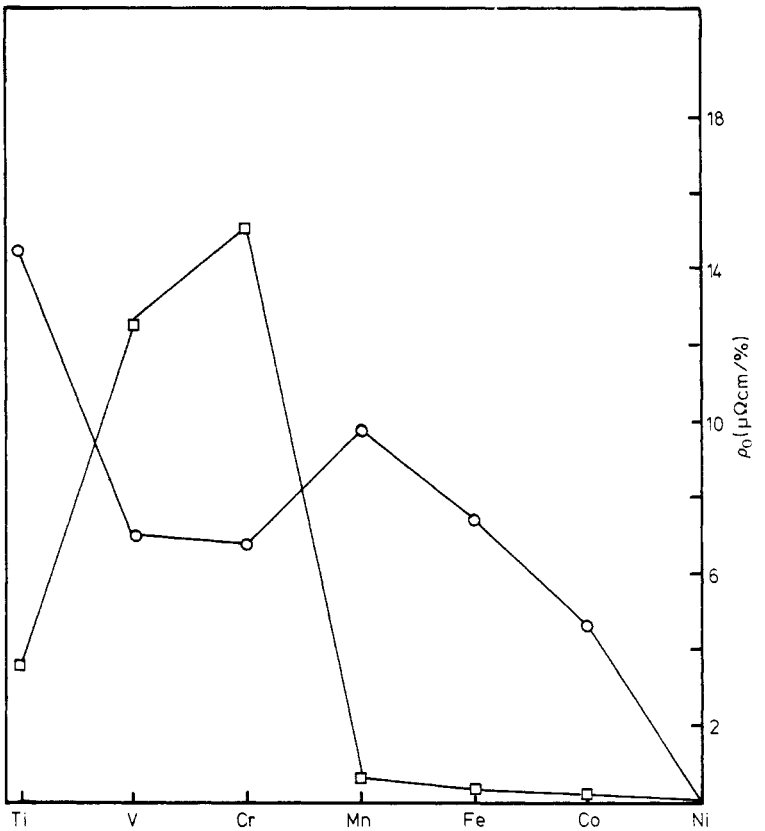

Figure 2. The resistivity of 3d impurities in nickel for each spin direction. □, $\rho_{0\uparrow}$; ○, $\rho_{0\downarrow}$.

are also listed in table 1 and are plotted on figure 2. These results are in approximate agreement with those derived by Leonard *et al* (1969) and by Dorleijn and Miedema (1975) from the residual resistivity of ternary alloys.

The interpretation of the resistivities $\rho_{0\uparrow}$ and $\rho_{0\downarrow}$ of 3d impurities (figure 2) on the basis of the Friedel model (Friedel 1967) is well known. We shall describe it briefly.

When the difference in the number of 3d electrons between the nickel and the impurity is large (Cr, V, Ti) a spin ↑ d bound state is repelled above the spin ↑ d band. This explains, for instance, that the magnetic moment of Cr, V or Ti impurities is opposite to the nickel moment. The resonance of the $s_\uparrow$ electrons with the bound state (formation of a virtual bound state) explains the peak of $\rho_{0\uparrow}$ around Cr (figure 2). For **Ni**Cr one can deduce from the change in magnetic moment ($d\mu/dC \simeq -4\,\mu_B$ after Collins and Low 1965) that the centre of the virtual bound state (VBS) is above E_F and that only one of the five d↑ states is occupied. The phase shift of the spin ↑ d partial waves at E_F is then $\eta_2 = \pi/5$ and for 0·3 conduction electrons per atom and per spin direction, the expected resistivity per at% is

$$\rho_{0\uparrow} = 10^{-2} \times \frac{20\pi\hbar}{nk_F} \sin^2 \eta_2 \simeq 41\,\mu\Omega\,\text{cm}$$

The experimental value appears somewhat lower: 16·1 μΩ cm.

For V and Ti, $\rho_{0\uparrow}$ remains rather large, which seems to show that, even for Ti, the VBS is not repelled well above the Fermi level, in agreement with the conclusions of the work of Caudron *et al* (1973) on the specific heat of Ni based alloys.

For Co, Fe and Mn impurities $\rho_{0\uparrow}$ is very small. This is due to the presence of only s states at E_F for the spin $\uparrow$ direction and, in the absence of resonance effects, to the weakness of s–s scattering.

The resistivities $\rho_{0\downarrow}$ are fairly large for all the impurities, which certainly results from the high density of s and d states at E_F for the spin $\downarrow$ direction and from the resulting strong scattering of the spin $\downarrow$ electrons in these states.

5. Variation of the resistivity of binary nickel based alloys with temperature

5.1. Dependence on temperature expected from the two current model

At finite temperature T, the resistivity ρ_σ for the current of spin σ electrons can be written as the sum of residual and T dependent terms:

$$\rho_\sigma = \rho_{0\sigma} + \rho_{i\sigma}(T). \tag{20}$$

In addition the occurrence of spin non-conserving scattering can be expressed by a spin-mixing resistivity $\rho_{\uparrow\downarrow}(T)$. We suppose $\rho_{\uparrow\downarrow}(0) = 0$ (we have discussed this assumption at the end of §2). One derives from (13):

$$\rho(T) = \frac{[\rho_{0\uparrow} + \rho_{i\uparrow}(T)][\rho_{0\downarrow} + \rho_{i\downarrow}(T)] + \rho_{\uparrow\downarrow}(T)[\rho_{0\uparrow} + \rho_{i\uparrow}(T) + \rho_{0\downarrow} + \rho_{i\downarrow}(T)]}{\rho_{0\uparrow} + \rho_{i\uparrow}(T) + \rho_{0\downarrow} + \rho_{i\downarrow}(T) + 4\rho_{\uparrow\downarrow}(T)}. \tag{21}$$

In principle, using sets of alloys of different concentrations, the different parameters can be estimated independently at each temperature (see Appendix). We will limit the discussion here to the more qualitative aspects.

In the temperature range where the residual resistivities $\rho_{0\uparrow}$ and $\rho_{0\downarrow}$ are much larger than $\rho_{i\uparrow}(T)$, $\rho_{i\downarrow}(T)$ and $\rho_{\uparrow\downarrow}(T)$ (e.g. $T \lesssim 45$ K for $\rho_0 \simeq 1\ \mu\Omega$ cm) one can limit the expression (21) to the terms of first order in $\rho_{i\sigma}(T)$ and $\rho_{\uparrow\downarrow}(T)$. One obtains

$$\rho_T(T) = \rho(T) - \rho_0 = \left(1 + \frac{(\alpha - \mu)^2}{(1 + \alpha)^2\mu}\right)\rho_i(T) + \frac{(\alpha - 1)^2}{(\alpha + 1)^2}\rho_{\uparrow\downarrow}(T) \tag{22}$$

where:

(i) ρ_0 is the residual resistivity ($\rho_0 = \rho_{0\downarrow}\rho_{0\downarrow}/(\rho_{0\uparrow} + \rho_{0\downarrow})$) and $\alpha = \rho_{0\downarrow}/\rho_{0\uparrow}$.

(ii) $\rho_i(T)$ is defined by

$$\rho_i(T) = \frac{\rho_{i\uparrow}(T)\rho_{i\downarrow}(T)}{\rho_{i\uparrow}(T) + \rho_{i\downarrow}(T)}$$

and

$$\mu = \rho_{i\downarrow}(T)/\rho_{i\uparrow}(T).$$

The temperature dependent scattering (by phonons and magnons) is then characterized by $\rho_{\uparrow\downarrow}(T)$, $\rho_i(T)$ and μ. The parameter μ should vary slowly with the temperature and, in a first approximation, will be supposed constant in the helium temperature range. We point out that $\rho_i(T)$ is not the resistivity ρ_T of the pure metal ($\rho_T = \rho(T) - \rho_0$). Actually the resistivity ρ_T of a 'pure' ferromagnetic metal is very

indirectly linked to $\rho_i(T)$. First, in metals of usual purity, the dominant scattering in the helium temperature range is the scattering by the residual impurities and the resistivity ρ_T should depend on the impurity type in the same way as that of definite alloys. Secondly the resistivity of pure ferromagnetic metals is enhanced (Schwerer and Silcox 1968) by the magnetoresistance effect in the internal induction ($4\pi M$ + demagnetizing field); from Kohler's rule this enhancement vanishes for concentrated alloys. Both mechanisms certainly explain the very wide spread of the experimental data for the resistivity of pure nickel at low temperature: from $14 \times 10^{-12} T^2$ Ω cm (Schwerer and Silcox 1968) to $26 \times 10^{-12} T^2$ Ω cm (White and Tainsh 1967). After correction for the enhancement by magnetoresistance, Schwerer and Silcox (1968) find $9{\cdot}5 \times 10^{-12} T^2$ Ω cm. It turns out that the resistivity of the pure metal can be only of little help in determining $\rho_i(T)$. We shall rather consider $\rho_i(T)$ as an unknown function to determine from the data on the resistivity of dilute alloys.

Expression (22) predicts that, at low temperature, ρ_T (or the deviation from MR) depends on the type of impurities in solution (*via* α) but not on their concentration. If the residual spin-mixing term $\rho_{\uparrow\downarrow}(0)$ cannot be neglected (low resistivity alloys) it can be shown (Jaoul and Campbell 1975) that the expression (22) for the resistivity at low temperature still holds, provided that α is replaced by a concentration dependent α'

$$\alpha' = \frac{\rho_{0\downarrow} + 2\rho_{\uparrow\downarrow}(0)}{\rho_{0\uparrow} + 2\rho_{\uparrow\downarrow}(0)}.$$

At high temperatures (room temperature and above), if $\rho_{i\uparrow}(T)$, $\rho_{i\downarrow}(T)$ and $\rho_{\uparrow\downarrow}(T)$ dominate $\rho_{0\uparrow}$ and $\rho_{0\downarrow}$, the main contribution of the impurities arises from terms of first order in $\rho_{0\uparrow}$ and $\rho_{0\downarrow}$ in the development of (21), and so the deviations from MR are predicted to be proportional to the impurity concentration.

Finally, as the Curie temperature is approached, other effects will come into play which we do not discuss here.

5.2. *General features of the experimental deviations from Matthiessen's rule*

5.2.1. A typical behaviour of the deviations is shown on figure 3 for two **NiCr** alloys; the deviations are observed to be independent of concentration at low temperature and approximately proportional to the concentration at high temperature. The two current model prediction is thus obeyed.

5.2.2. The deviations at low temperature are nearly concentration independent in a wide concentration range but begin to drop for alloys of low residual resistivity (figure 4). This effect has already been observed in **NiCu** alloys by Greig and Rowlands (1974) and can be explained by a zero temperature spin-mixing $\rho_{\uparrow\downarrow}(0)$ (Jaoul and Campbell 1975). We will consider as far as possible only the concentration range where the deviations are nearly independent of the concentration.

5.2.3. **NiMn** is a special case: one observes in figure 4 that $\rho_\uparrow$ increases regularly with the concentration. An additional mechanism for deviation from MR certainly occurs (Mills *et al* 1971, Rowlands 1973). But, even for **NiMn**, there is a range of residual resistivity ($0{\cdot}3\ \mu\Omega\,\text{cm} < \rho_0 < 0{\cdot}7\ \mu\Omega\,\text{cm}$) where the deviations from MR depend relatively little on the concentration and can be explained by a two current conduction.

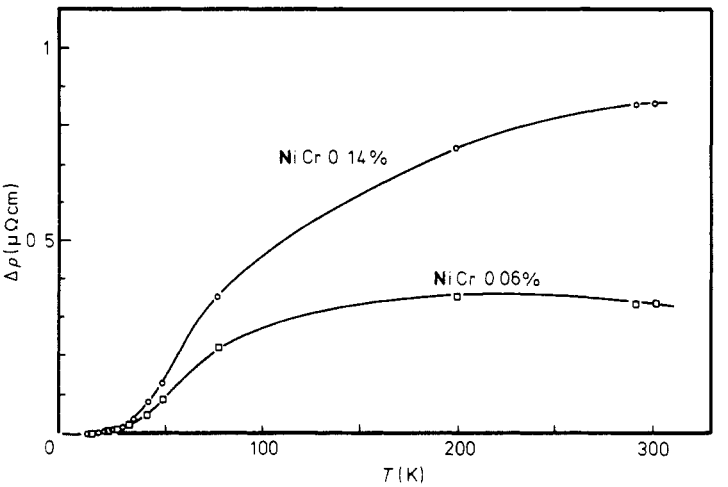

Figure 3. The deviation from Mattheissen's rule against the temperature for two NiCr alloys.

5.3. Resistivity of nickel based alloys at low temperature

We only consider the experimental data in the range of residual resistivity where ρ_T (that is $\rho(T) - \rho_0$) is, at least approximately, independent of the impurity concentration (figure 4). For **NiCo**, **NiFe**, **NiMn**, **NiCr**, **NiV** and **NiCrMn** alloys, we have obtained a good fit of the experimental data with the expression (22) of $\rho_\uparrow$ by taking:

(i) the values of α derived from the measurements on ternary alloys (§4) and listed in table 1 (for **Ni** + 0·07 at% Cr + 0·2 at% Mn the effective value of α calculated from table 1 is 1·5).

(ii) $\mu = 3{\cdot}6$.

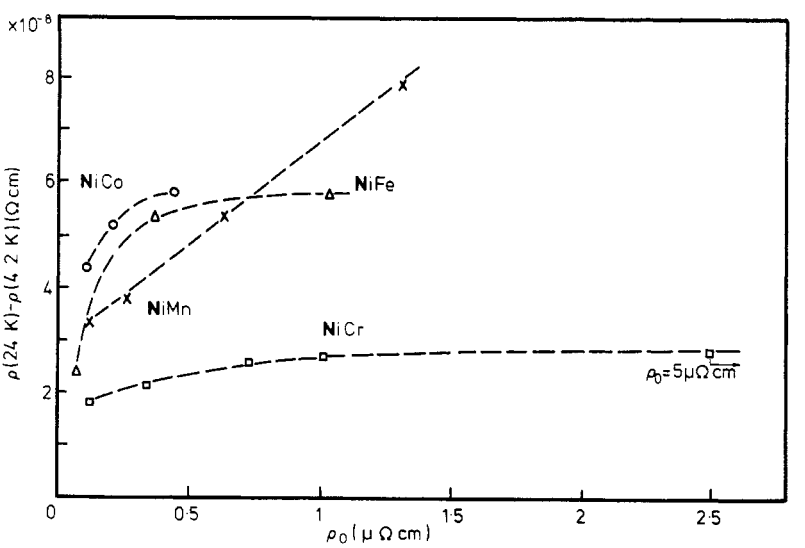

Figure 4. The resistivity increase between 4·2 K and 24 K against the concentration for several types of alloys.

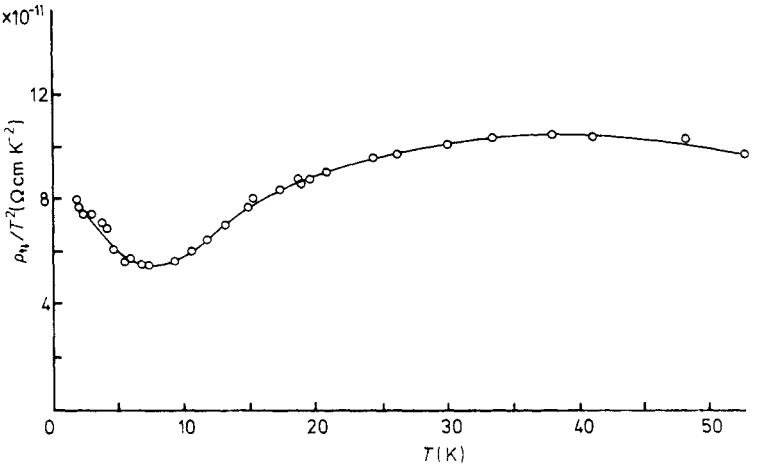

Figure 5. The ratio of $\rho_{\downarrow}(T)$ to T^2 against T for Ni. The circles correspond to values obtained using equation (22) and data from Ni + 3 at% Fe. The curve corresponds to the function $\rho_{\uparrow\downarrow}(T)$ which has been adopted for the interpretation of the experimental results for all the nickel based alloys.

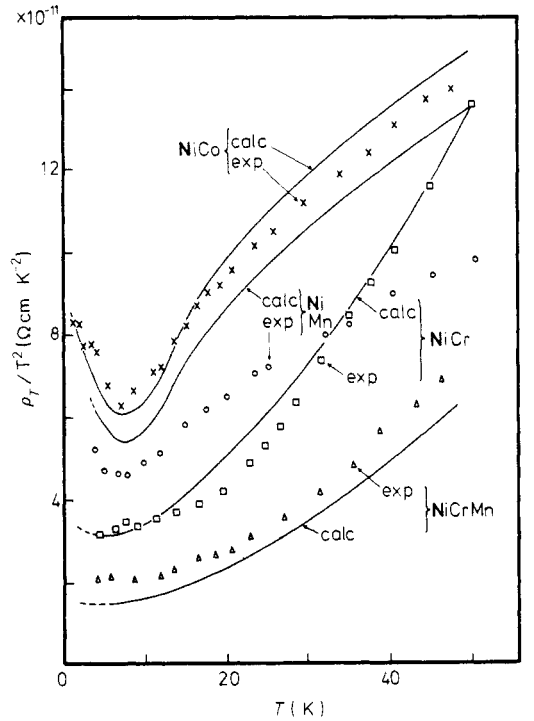

Figure 6. The ratio ρ_T/T^2 is plotted against T for: ×, Ni + 3 at% Co (ρ_0 = 0·44 μΩ cm); ○, Ni + 0·4 at% Mn (ρ_0 = 0·25 μΩ cm); □, Ni + 0·14 at% Cr (ρ_0 = 0·73 μΩ cm) and △, Ni + 0·07 at% Cr + 0·2 at% Mn (ρ_0 = 0·82 μΩ cm). The full lines have been calculated from expression (22) with the parameters indicated in the text.

(iii) $\rho_i(T) = 9{\cdot}5 \times 10^{-12}T^2 + 1{\cdot}7 \times 10^{-14}T^4$ (in Ω cm if T in K).

(iv) the spin-mixing resistivity $\rho_{\cdot\downarrow}(T)$ which yields an accurate fit for the alloy Ni + 3 at% Fe. The function $\rho_{\uparrow\downarrow}(T)/T^2$ is shown on figure 5.

On figure 6 we have plotted the experimental and calculated values of ρ_T/T^2 for **Ni**Co, **Ni**Mn, **Ni**Cr and **Ni**CrMn alloys (a plot of ρ_T/T^2 instead of ρ_T appeared more convenient; the figure does not include the plots for **Ni**Fe and **Ni**V which are little different from those for **Ni**Co and **Ni**Cr respectively). The model explains why ρ_T becomes very large when α is very different from unity, that is for **Ni**Co ($\alpha \simeq 30$), **Ni**Fe ($\alpha \simeq 20$), **Ni**Mn ($\alpha \simeq 15$); this comes from the term $(\alpha - 1)^2/[(\alpha + 1)^2]\rho_{\cdot\downarrow}(T)$ in expression (22). The model also explains the very different form of temperature dependence of ρ_T/T^2 according to whether $\alpha \lesssim 1$ or $\alpha \gg 1$. For $\alpha < 1$ or $\alpha \simeq 1$ (**Ni**Cr, **Ni**CrMn and also **Ni**V not plotted on figure 6) with $\mu = 3{\cdot}6$, the dominant term in (22) is $\{1 + [(\alpha - \mu)^2/(1 + \alpha)^2\mu]\}\rho_i(T)$ and the temperature dependence of ρ_T reflects that of $\rho_i(T)$; on the contrary for $\alpha \gg 1$ (**Ni**Co, **Ni**Fe, **Ni**Mn) the dominant term in (22) is $[(\alpha - 1)^2/(\alpha + 1)^2]\rho_{\uparrow\downarrow}(T)$ and the temperature dependence of ρ_T reflects that of $\rho_{\cdot\downarrow}(T)$. We note that the calculated curves reproduce fairly well the features of the experimental plot: curvature, crossing of the curve of **Ni**Cr with those of **Ni**Mn and **Ni**Co etc. The experimental curves for **Ni**Mn and **Ni**CrMn are somewhat below the calculated curves but these alloys are less concentrated and we believe that the discrepancy can be mostly ascribed to the $\rho_{\uparrow\downarrow}(0)$ mechanism.

5.4. *Need for spin-mixing*

It has been suggested by Greig and Rowlands (1974) that the temperature dependence of the resistivity of Ni based alloys could as well be explained in a model with two independent currents (without spin-mixing). According to these authors, the experimental data could be explained by the first term of (22) alone

$$\rho_T = \left(1 + \frac{(\alpha - \mu)^2}{(1 + \alpha)^2\mu}\right)\rho_i(T). \tag{23}$$

A value of μ much smaller than 1 is then needed to explain the high values of ρ_T for **Ni**Co, **Ni**Fe, **Ni**Mn ($\alpha \gg 1$) and also its rather high value for **Ni**Cr ($\alpha < 1$). Thus, Greig and Rowlands (1974) obtained a reasonable agreement with their experimental data for **Ni**Fe and **Ni**Cr with $\mu = 0{\cdot}2$, $\alpha_{Fe} = 8$, $\alpha_{Cr} = 0{\cdot}8$. We have several objections to this interpretation:

(i) With $\mu = 0{\cdot}2$ the expression (23) predicts that ρ_T of **Ni**CrMn alloys should progressively increase from **Ni**Cr to **Ni**Mn (as $0{\cdot}2 < \alpha_{(\ldots)} < \alpha_{Mn}$). This is in contradiction to our observation for **Ni**CrMn of a resistivity ρ_T definitely smaller than that for **Ni**Cr and **Ni**Mn.

(ii) Greig and Rowlands (1974) took $\rho_i(T)$ equal to the resistivity of a pure nickel specimen ($15 \times 10^{-12}T^2$ Ω cm in the low temperature limit). But Schwerer and Silcox (1967) have shown that the resistivity of pure nickel is enhanced by a magnetoresistance effect in the internal induction and they found that the resistivity of nickel in zero induction would be definitely lower ($\rho_{Ni}(B = 0) = 9{\cdot}5 \times 10^{-12}T^2$ at low temperature). As the effect of internal induction can be neglected in alloys (on account of Kohler's rule), the term $\rho_i(T)$ in expressions (22) or (23) is to be taken in zero induction and should not exceed the resistivity $\rho_{Ni}(B = 0)$ found by Schwerer and

Silcox. A choice of $\rho_i(T)$ smaller than $\rho_{Ni}(B = 0)$ leads to larger values of $\rho_T/\rho_i(T)$ which cannot be explained by expression (23).

(iii) The values of α estimated on the zero spin-mixing assumption, particularly the value for Cr, are incompatible with values obtained from the ternary alloy data (see §4 and the Appendix).

5.5. *Interpretation of the spin-mixing term*

It has been shown that the spin-mixing could not be due to collisions between electrons with opposite spins but should be ascribed to electron–magnon collisions (Fert 1969, Mills *et al* 1971). The contribution from the electron–magnon collisions has been calculated on an s–d model and can be written

$$\rho_{\uparrow\downarrow}(T) = \frac{3\pi}{8}\frac{mSJ^2k_BT}{Ne^2\hbar\epsilon_F Dk_F^2} f\left(\frac{\epsilon_m}{k_BT}\right)$$

where

$$f(x) = \left(\frac{x}{1-e^{-x}} - \lg(e^x - 1)\right) = \begin{cases} -\ln x, & x \ll 1 \\ xe^{-x}, & x \gg 1. \end{cases}$$

S is the spin of the d local moment, J the constant of the s–d exchange, D the spin-wave stiffness constant, $\epsilon_m = \hbar Dq_1^2$ where q_1 is the gap between the spin $\uparrow$ and spin $\downarrow$ Fermi surfaces in k space (in the calculation q_1 is considered constant but should actually correspond to a mean value of the gap).

The function $\rho_{\uparrow\downarrow}(T)/T^2$ has a broad maximum (Fert 1969) at $T \simeq \epsilon_m/k_B$ and this maximum could correspond to that observed on the experimental plot of $\rho_{\uparrow\downarrow}/T^2$ (figure 5). Taking D from Shirane *et al* (1968), $S = 0{\cdot}3$, $SJ = 0{\cdot}12$ eV, $\epsilon_F = 5{\cdot}4$ eV, $q_1 = \frac{1}{20}k_F$ one finds:

$$\epsilon_m/k_B = 17\ \text{K}$$

with a value of $\rho_{\uparrow\downarrow}/T^2$ at the maximum

$$(\rho_{\uparrow\downarrow}/T^2)_{max} = 0{\cdot}38 \times 10^{-14}\ \Omega\,\text{cm}\ (T \text{ in K}).$$

In comparison the maximum of $\rho_{\uparrow\downarrow}/T^2$ on the experimental plot of figure 5 is about 10^{-14} Ω cm and occurs at about 40 K.

At low temperature the model with two spin $\uparrow$ and spin $\downarrow$ Fermi surfaces separated by q_1 predicts an exponential decrease of $\rho_{\uparrow\downarrow}(T)$ as $\exp[-\epsilon_m/k_BT]$. In contrast, if

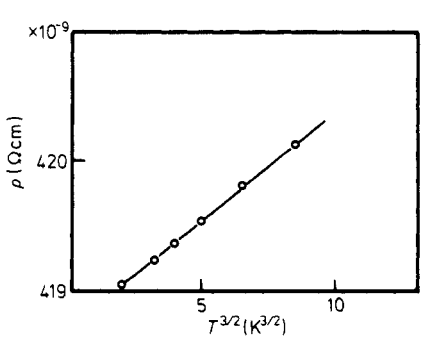

Figure 7. Resistivity of a NiCo 3 at% alloy against $T^{3/2}$.

Table 2. Experimental and calculated deviations from MR in several nickel base alloys at 77 K, 200 K and 300 K [$\Delta\rho$ = ρ (alloy) − ρ (residual) − ρ (pure Ni)].

Alloy	Residual Resistivity $\rho_0(\mu\Omega\,\text{cm})$	77 K		200 K		300 K	
		$(\Delta\rho/\rho_0)_{cal}$	$(\Delta\rho/\rho_0)_{exp}$	$(\Delta\rho/\rho_0)_{cal}$	$(\Delta\rho/\rho_0)_{exp}$	$(\Delta\rho/\rho_0)_{cal}$	$(\Delta\rho/\rho_0)_{exp}$
NiCo3at%	0·44	1·02	1·00	2·27	2·43	3·11	3·38
NiFe3at%	1·04	0·44	0·44	1·19	1·25	1·77	1·70
NiMn1at%	0·63	0·54	0·51			1·24	1·49
NiCr1at%	4·96	0·14	0·138	0·44	0·46	0·58	0·60
NiCr0·14at%	0·73	0·42	0·47	0·50	0·90	0·75	0·95

one supposes that the spin ↑ and spin ↓ Fermi surfaces touch or are very near in some places, a $T^{3/2}$ law is expected. The experimental results support the second hypothesis: the upturn of $\rho_{\uparrow\downarrow}/T^2$ below 10 K corresponds approximately to a $T^{3/2}$ dependence at low temperature. It can be checked on figure 7 that the temperature dependence of ρ_T for **Ni**Fe is actually very little different from a $T^{3/2}$ dependence.

We conclude that collisions with spin-waves can explain the order of magnitude of $\rho_{\uparrow\downarrow}(T)$ but that a precise interpretation of the variation of $\rho_{\uparrow\downarrow}(T)$ with T is very problematic.

5.6. Deviations from Matthiessen's rule at 77 K, 200 K and 300 K

The deviations from MR at 77 K, 200 K and 300 K for several alloys (table 2) have been compared to the deviations calculated from expression (21). The impurity parameters ($\rho_{0\uparrow}$, $\rho_{0\downarrow}$) being those derived from the residual resistivity of ternary alloys (table 1), the best fit is obtained with the host parameters [μ, $\rho_i(T)$, $\rho_{\uparrow\downarrow}(T)$] listed in table 3. The agreement between experimental and calculated deviations (table 2) is reasonably good but the determination of μ, $\rho_i(T)$ and $\rho_{\uparrow\downarrow}(T)$ does not turn out to be very accurate; sets of parameters in which μ is increased somewhat while $\rho_{\uparrow\downarrow}(T)$ is decreased (or vice versa) give almost as good fits. We find μ always larger than 1, which could be due, independently of the scattering mechanisms, to the lighter effective masses of the spin ↑ electrons. It appears also that the spin-mixing term $\rho_{\uparrow\downarrow}(T)$, up to 300 K, does not become much larger than $\rho_i(T)$ and that, at RT, the two currents are not yet completely mixed.

6. Resistivity of iron based alloys

We have measured the resistivity of **Fe**Ni (C = 1 and 2 at%), **Fe**Mn (C = 1·4 and 1·9 at%), **Fe**Cr (C = 0·3 and 0·6 at%) between 1·5 K and 300 K and the resistivity

Table 3. Values of the parameters μ, $\rho_i(T)$, $\rho_{\uparrow\downarrow}(T)$ which have been used to interpret the deviations from MR at 77 K, 200 K, 300 K in nickel based alloys.

Temperature	$\rho_{\uparrow\downarrow}(T)$ ($\mu\Omega$ cm)	$\rho_i(T)$ ($\mu\Omega$ cm)	μ	$\rho_{i\uparrow}(T)$ ($\mu\Omega$ cm)	$\rho_{i\downarrow}(T)$ ($\mu\Omega$ cm)
77	0·9 ± 0·3	0·32	5 ± 1	0·38	1·9
200	5 ± 2	2·5	5 ± 2	3	15
300	11 ± 4	5·4	4 ± 2	6·7	27

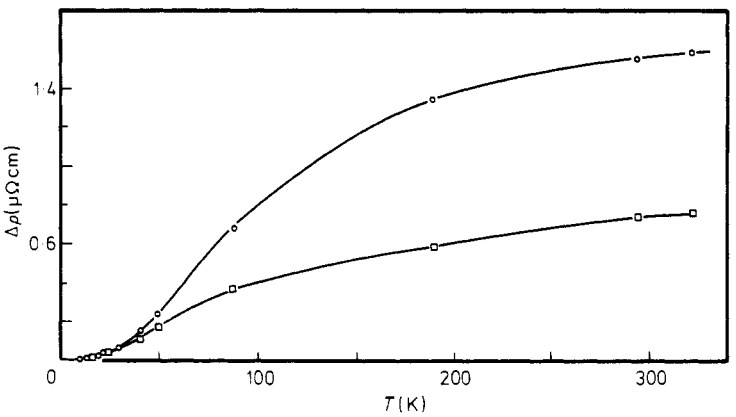

Figure 8. Deviation from Matthiessen's rule against T for two **Fe**Cr alloys: ○, **Fe**Cr 0·6% and □, **Fe**Cr 0·3%.

of **Fe**Ti (C = 1 at%), **Fe**V (C = 1·8 at%), **Fe**Co (C = 1 at%), **Fe**Si (C = 1 at%) at 4·2 K and 293 K. The results for the room temperature deviations are in good agreement with those of Arajs *et al* (1969).

The main features of the deviations from MR are similar to those of Ni based alloys. Figure 8 shows the deviations from MR for two **Fe**Cr alloys: one observes that the deviations are approximately independent of the concentration C below 30 K and proportional to C at room temperature. The same behaviour is observed for **Fe**Mn and **Fe**Ni alloys.

Figure 9 shows $\rho_T(\rho_T = \rho(T) - \rho_0)$ at low temperature for two **Fe**Cr alloys (0·3 and 0·6 at%) and pure Fe. The resistivity ρ_T of the **Fe**Cr alloys turns out to be about five times the resistivity of pure iron and nearly the same for the two alloys. We however have only studied two alloys for each type of impurity and we do not know if ρ_T remains approximately independent of C in a wider concentration range. Figure 10 shows the resistivity ρ_T of **Fe**Mn, **Fe**Ni alloys and pure Fe: for **Fe**Mn ρ_T is larger than the resistivity of pure iron by about a factor of six and for **Fe**Ni only a little larger.

These main features of ρ_T for the Fe based alloys suggest that the measurements can be interpreted in a two-current model, as for the Ni based alloys. However we have not measured the residual resistivities of ternary alloys† to determine independently the ratios α of the impurities, and all the parameters of the two current model $[\alpha, \mu, \rho_i(T), \rho_{\downarrow}(T)]$ must be derived from the data on binary alloys only. We have tentatively chosen $\mu = 1$, which seems a reasonable value as the spin ↑ and spin ↓ densities of states at the Fermi level are not very different in the conduction band of iron. We have also assumed $\rho_i(T) = \rho$ (pure Fe) without correction for the magnetoresistance effect in the internal field. We then obtained the best fit between the experimental and calculated (from expression 22) values of ρ_1 at low temperature with

$$\alpha_{Cr} = \tfrac{1}{11} \text{ (or 11)} \qquad \alpha_{Mn} = \tfrac{1}{6} \text{ (or 6)} \qquad \alpha_{Ni} = 3 \text{ (or } \tfrac{1}{3}).$$

It can be checked on figure 11 that the fit of expression (22) to the experimental data for **Fe**Cr and **Fe**Mn yield very nearly the same values of $\rho_{\uparrow\downarrow}(T)$. We keep

† Except a few measurements reported in a previous paper (Campbell *et al* 1967).

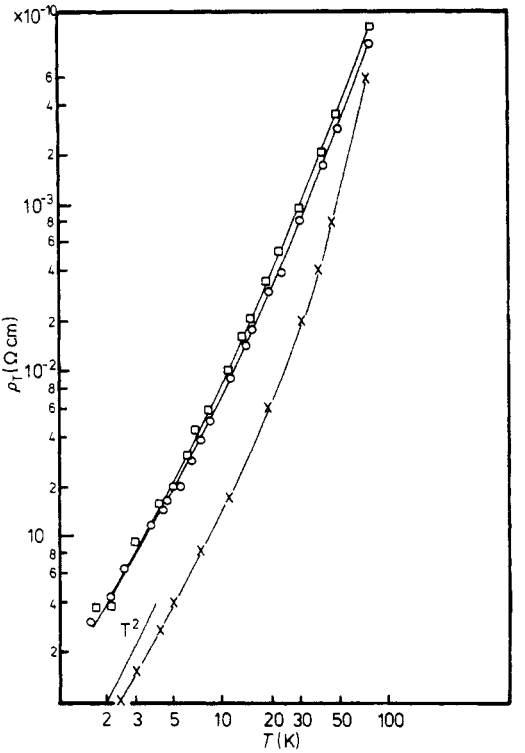

Figure 9. Temperature dependent part of the resistivity against T for: ○, **Fe**Cr 0·3% and □, **Fe**Cr 0·6% alloys and ×, pure iron at low temperature (logarithmic plot).

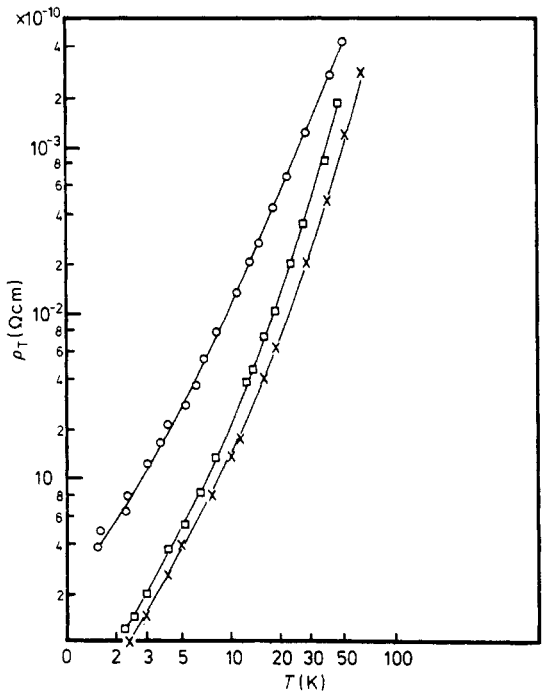

Figure 10. Temperature dependent part of the resistivity against T for: ○, FeMn; □, FeNi alloys and ×, pure Fe (logarithmic plot).

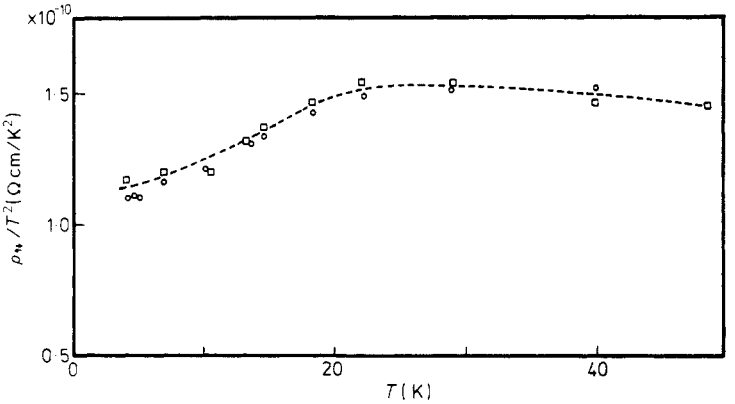

Figure 11. $\rho_{\downarrow}(T)/T^2$ against T for Fe. The circles and the squares correspond to the values of $\rho_{\uparrow,\downarrow}(T)$ which fit expression (22) with the experimental data for, respectively, FeMn and FeCr alloys.

the values $\alpha_{Cr} = \frac{1}{11}$, $\alpha_{Mn} = \frac{1}{6}$, $\alpha_{Ni} = 3$ which agree better with the Friedel model for ferromagnetic transition alloys than the inverse values.

The deviations from MR at room temperature for **FeCr**, **FeMn** and **FeNi** alloys are listed in table 4. The impurity resistivity of these alloys being definitely smaller than their thermal resistivity at RT, the deviation from MR at RT is predicted by the two current model (with $\mu = 1$) to be approximately:

$$\frac{\Delta\rho_{RT}}{\rho_0} = \frac{(\alpha - 1)^2}{4\alpha}. \tag{24}$$

The values of $\Delta\rho_{RT}/\rho_0$ have been calculated with $\alpha_{Cr} = \frac{1}{11}$, $\alpha_{Mn} = \frac{1}{6}$, $\alpha_{Ni} = 3$ and are listed in table 4. The agreement with the experimental values is fairly good.

For **FeTi**, **FeV**, **FeCo**, **FeSi**, the only data are the deviations from MR at RT: $\Delta\rho/\rho_0 = 0{\cdot}58$ for **FeTi** (1 at%), $\Delta\rho/\rho_0 = 1{\cdot}5$ for **FeV** (1·8 at%) $\Delta\rho/\rho_0 \lesssim 0$ for **FeCo** (1 at%), $\Delta\rho/\rho_0 \lesssim 0$ for **FeSi** (1 at%). Assuming $\Delta\rho/\rho_0$ at RT given by expression (24), we have derived the values of α for each impurity. The values of α (after a choice between α and α^{-1}), $\rho_{0\uparrow}$, $\rho_{0\downarrow}$ are listed in table 5. The resistivities $\rho_{0\uparrow}$ and $\rho_{0\downarrow}$ are plotted on figure 11.

The results of table 5 or figure 11 can be interpreted in the Friedel model for the ferromagnetic transition alloys. Friedel (1967) showed that, in the case of an unfilled d band and of a repulsive potential, resonance effects occur if the Fermi

Table 4. Experimental and calculated deviations from MR in several iron based alloys at 77 K, 200 K and 300 K [$\Delta\rho$ = ρ (alloy) − ρ (residual) − ρ (pure Fe)].

Impurity	Cr		Mn		Ni	
Concentration (at%)	0·3	0·6	1·4	1·9	1	2
Residual resistivity (μΩ cm)	0·8	1·5	2·4	3·2	1·9	2·6
$(\Delta\rho/\rho_0)_{exp}$	0·82	0·99	2·14	2·02	0·47	0·38
$(\Delta\rho/\rho_0)_{cal} = (\alpha - 1)^2/4\alpha$	1·04		2·27		0·33	

Table 5. The residual resistivity per at%, the parameter $\alpha = \rho_{0\downarrow}/\rho_{0\uparrow}$ and the spin ↑ and spin ↓ residual resistivities per at% for impurities in iron.

Impurity	Ti	V	Cr	Mn	Co	Ni
Resistivity						
ρ_0(μΩ cm/at%)	2·9	1·4	2·6	1·7	2	1·8
$\alpha = \rho_{0\downarrow}/\rho_{0\uparrow}$	$\frac{1}{4}$	$\frac{1}{8}$	$\frac{1}{6}$	$\frac{1}{11}$	1	3
$\rho_{0\uparrow}$(μΩ cm/at%)	14·5	13·5	18	21	2·0	2·4
$\rho_{0\downarrow}$(μΩ cm/at%)	3·6	1·6	3	1·9	2·0	7·2

level is just below the top of the band. For iron the Fermi level is just below the top of the spin ↑ d band and repulsive potentials (Mn, Cr, V, Ti impurities) push up a spin ↑ d virtual bound state in the d band through the Fermi level; this explains the progressive lowering of the magnetic moment for Mn, Cr, V and Ti impurities. If we consider the transport properties, a strong s↑–d↑ scattering should be associated with the high density of spin ↑ d states at the Fermi level for repulsive potentials. This is the explanation of the high value of $\rho_{0\uparrow}$ for Mn, Cr, V and Ti impurities (figure 12).

A resonance effect at the spin ↑ Fermi level is not expected for an attractive potential (Friedel 1967), which explains why for Co or Ni impurities, $\rho_{0\uparrow}$ is much lower than for Mn, Cr, V or Ti.

For the spin ↓ electrons, the Fermi level is in the middle of the d band, so that resonance effects are not expected for the spin ↓ direction. This is consistent with the low values of $\rho_{0\downarrow}$ for the 3d impurities.

7. Conclusion

We have discussed in detail the two band model for conduction in ferromagnetic metals, and have shown that the formula for the two band model including mixing

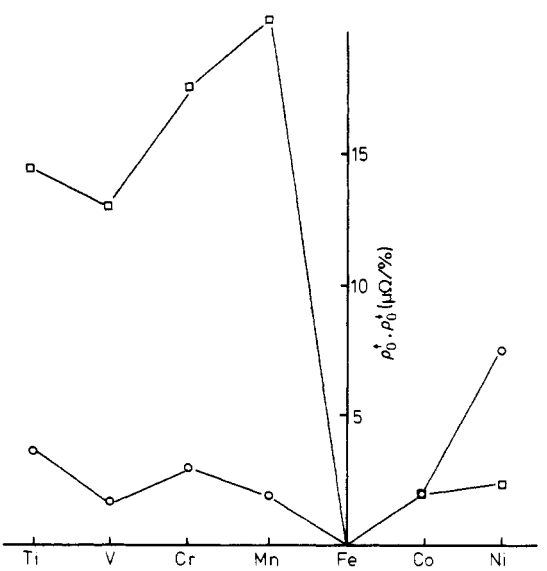

Figure 12. The resistivity of 3d impurities in iron for each spin direction: □, $\rho_{0\uparrow}$; ○, $\rho_{0\downarrow}$. α for Ti = $\frac{1}{4}$, V = $\frac{1}{8}$, Cr = $\frac{1}{6}$, Mn = $\frac{1}{11}$, Co ≃ 1 and Ni ≃ 3.

(equation 22) is of rather general validity. This puts the model, which has been widely used in interpreting experimental data, on a firmer theoretical footing.

We then presented experimental data for the temperature dependence of the resistivity of binary Ni and Fe based alloys and for the deviations from Matthiessen's rule at low temperature in ternary Ni based alloys. The results were analysed to give consistent values of the parameters $\alpha = \rho_{\downarrow}^{0}/\rho_{\uparrow}^{0}$ for each impurity. These values follow the qualitative predictions of the s–d model. We also obtain temperature dependent pure metal intra-spin-band and spin-mixing scattering rates.

Appendix

The parameters of the two current model can be extracted from the experimental results in an unambiguous manner by an appropriate analysis of the data, as long as sufficient carefully determined points exist.

The simplest case is that of ternary alloys at low temperatures assuming zero spin mixing (this is a reasonable approximation when the total impurity resistivity is greater than 1 μΩ cm for all samples). Equation (19) can be rewritten

$$\frac{1}{a}\frac{\Delta\rho}{\rho_A} + \frac{1}{b}\frac{\Delta\rho}{\rho_B} = 1 \tag{A1}$$

with

$$\begin{aligned} a &= (\alpha_A - \alpha_B)^2/\alpha_B(1 + \alpha_A)^2 \\ b &= (\alpha_A - \alpha_B)^2/\alpha_A(1 + \alpha_B)^2. \end{aligned} \tag{A2}$$

This is in fact the Kohler–Sondheimer–Wilson relation. A plot of $\Delta\rho/\rho_A$ against $\Delta\rho/\rho_B$ should give a straight line with intercepts a and b. When these values are determined, the simultaneous equations

$$\begin{aligned} \alpha_A &= [(a\alpha_B)^{1/2} + \alpha_B]/[1 - (a\alpha_B)^{1/2}] \\ \alpha_B &= [\alpha_A - (b\alpha_A)^{1/2}]/[(b\alpha_A)^{1/2} + 1] \end{aligned} \tag{A3}$$

can be solved graphically to give the values of α_A, α_B with their associated uncertainties.

As an example, we plot in figure 13 results for **Ni**MnCr alloys in the form of equation (A1). With the values of a and b obtained from this plot, ($a = 6$, $b = 2$) a graphical solution of equations (A3) is given in figure 14. We obtain unambiguously

$$\alpha_{Mn} = 11 \pm 2 \qquad \alpha_{Cr} = 0{\cdot}37 \pm 0{\cdot}05.$$

Our own data together with results in the literature have been analysed in this way to give the values for the different impurities.

A similar approach, including the possibility of spin-mixing can be used for binary alloys at non-zero temperature as pointed out by Schwerer and Conroy (1971). If there is zero spin-mixing at zero temperature and we define as usual

$$\Delta(T) = \rho_{alloy}(T) - [\rho_{alloy}(0) + \rho_{pure}(T)] \tag{A4}$$

then we can write

$$\frac{1}{a}\frac{\Delta(T)}{\rho(0)} + \frac{1}{b}\frac{\Delta(T)}{\rho_{pure}(T)} = 1 \tag{A5}$$

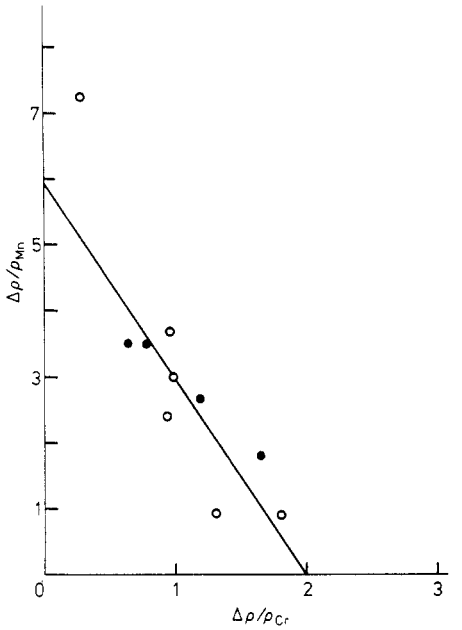

Figure 13. Deviations from Matthiessens rule for NiCrMn alloys plotted in the form of equation (A1). ○, present work; ●, Dorleijn and Miedema (1975).

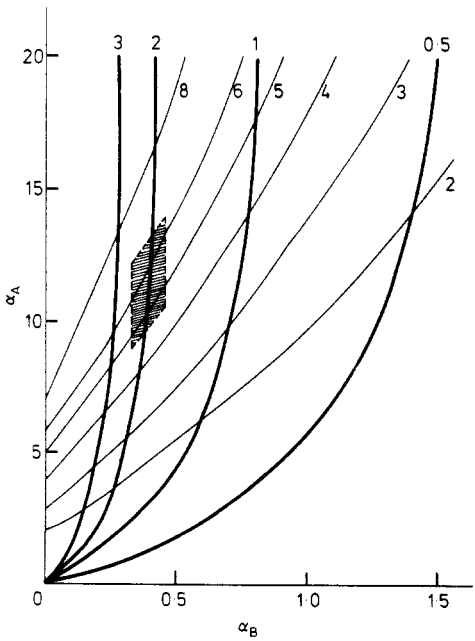

Figure 14. Graphic solutions of equations (A3). Hatched area corresponds to the range of possible values of a and b for the system NiMnCr estimated from figure 13. Heavy curves: equation (A3), fixed values of a. Light curves: equation (A3), fixed values of b.

with

$$a = \frac{[\alpha(1 + 2r) - (\mu + 2r)]^2}{\alpha[\mu + 1 + 4r]^2}$$
$$b = \frac{[\alpha(1 + 2r) - (\mu + 2r)]^2}{[\mu + r + \mu r][\alpha + 1]^2}. \tag{A6}$$

Here, α and μ are as defined in §5, $r = \rho_{\uparrow\downarrow}(T)/\rho^{\uparrow}_{\text{pure}}(T)$. Results at a fixed temperature for varying concentrations of two sets of binary alloys (impurity A and impurity B) give the four parameters α_A, α_B, μ and r. In fact, Schwerer and Conroy (1971) found that it was necessary to introduce zero temperature spin-mixing which means that the form (A4) is no longer valid. It is possible to return to this form by referring all measurements to a hypothetical 'unmixed' state. The corrections to be applied are

$$\Delta'(T) = \Delta(T) + \Delta_0$$

and

$$\rho'(0) = \rho(0) - \Delta_0$$

with

$$\Delta_0 = \tfrac{1}{2}\{[(\rho(0) - \rho_{\uparrow\downarrow}(0))^2 + 4\rho(0)\rho_{\uparrow\downarrow}(0)(\alpha - 1)^2/(\alpha + 1)^2]^{1/2} - |(\rho(0) - \rho_{\uparrow\downarrow}(0))|\}$$

Then if $\rho_{\uparrow\downarrow}(0)$ is chosen correctly, the relation (A5) should hold for the corrected parameters at each temperature.

References

Arajs S, Schwerer F C and Fischer R M 1969 *Phys. Stat. Solidi* **33** 731–40
Bourquart A, Daniel E and Fert A 1968 *Phys. Lett.* **26A** 260–3
Cadeville M C, Gautier F, Robert C and Roussel J 1969 *Solid St. Commun.* **7** 1701–4
Campbell I A, Fert A and Jaoul O 1970 *J. Phys. C: Solid St. Phys.* **3** 595–601
Campbell I A, Fert A and Pomeroy A R 1967 *Phil. Mag.* **15** 977–83
Caudron R, Caplain R, Meanier J J and Costa P 1973 *Phys. Rev.* B **8** 5247–56
Collins M F and Low G 1965 *Proc. Phys. Soc.* **86** 536–43
Dorleijn J F and Miedema A R 1975 *J. Phys. F: Metal Phys.* **5** 487–96
Durand J and Gautier F 1970 *J. Phys. Chem. Solids* **31** 2773–87
Farrel T and Greig D 1968 *J. Phys. C: Solid St. Phys.* **1** 1359–69
—— 1970 *J. Phys. C: Solid St. Phys.* **3** 138–45
Fert A 1969 *J. Phys. C: Solid St. Phys.* **2** 1784–8
Fert A and Campbell I A 1968 *Phys. Rev. Lett.* **21** 1190–2
—— 1971 *J. Phys. (Paris)* **32** suppl. C1 46–50
Fert A and Jaoul O 1972 *Phys. Rev. Lett.* **28** 303–7
Friedel J 1967 *Rendiconti della Scuala Internazionale di Fisica 'Enrico Fermi'* XXXVII Corso (New York: Academic Press)
Goy P and Grimes C C 1973 *Phys. Rev.* B **7** 299–306
Greig D and Rowlands J A 1974 *J. Phys. F: Metal Phys.* **4** 232–46
Jaoul O and Campbell I A 1975 *J. Phys. F: Metal Phys.* **5** L69–73
Leonard P, Cadeville M C, Durand J and Gautier F 1969 *J. Phys. Chem. Solids* **30** 2169–B
Loegel B and Gautier F 1971 *J. Phys. Chem. Solids* **32** 2723–35
Mills D L, Fert A and Campbell I A 1971 *Phys. Rev.* B **4** 196–201
Monod P 1968 *PhD Thesis* (Orsay)
Mott N F 1964 *Adv. Phys.* **13** 325
Price D C and Williams G 1973 *J. Phys. F Metal Phys.* **3** 810–24
Rowlands J A 1973 *J. Phys. F: Metal Phys.* **3** L149–53

Schwerer F C and Conroy J W 1971 *J. Phys. F: Metal Phys.* **1** 877–91
Schwerer F C and Silcox J 1968 *Phys. Rev. Lett.* **20** 101–3
Shirane G, Minkiewicz Y J and Nathans R 1968 *J. Appl. Phys.* **39** 383–8
Tsui D C 1971 *Phys. Rev.* **2** 669–83
Wang C S and Callaway J 1974 *Phys. Rev.* B **9** 4897–907
White G K and Tainsh R J 1967 *Phys. Rev. Lett.* **19** 105–6
Ziman J M 1960 *Electrons and Phonons* (Oxford: Clarendon Press) p 275